International Journal of Heat and Mass Transfer 52 (2009) 5020–5028

Contents lists available at ScienceDirect

International Journal of Heat and Mass Transfer

journal homepage: www.elsevier.com/locate/ijhmt

Bubble sweeping and interactions on wires during subcooled boiling

David M. Christopher *, Jun Jiang

Department of Thermal Engineering, Key Laboratory for Thermal Science and Power Engineering of Ministry of Education, Tsinghua University, Beijing 100084, China

ARTICLE INFO

Article history:
Received 6 July 2008
Received in revised form 10 April 2009
Accepted 27 April 2009
Available online 24 June 2009

Keywords:
Subcooled boiling
Bubble coalescence
Bubble motion

ABSTRACT

Multi-bubble dynamics on a heated wire are modeled with a phenomenological model of the temperature distributions around the bubbles and the forces acting on the bubbles. The model calculates the heat transfer from the wire to the bubble and the temperature distribution in the wire. The model balances the Marangoni force, the drag force, and the contact line force acting on the bubble to predict the bubble velocities. The predicted velocities and the predicted interactions agree well with experimentally observed bubble dynamics. The predictions show that when a moving bubble approaches a stationary bubble at moderate superheats, the reduced wire temperatures around the stationary bubble cause the moving bubble to slow and reverse direction before colliding with the stationary bubble. At higher superheats, the bubbles coalesce. The model also shows that when two bubbles approach each other from opposite directions, they will collide and coalesce at lower superheats than when only one bubble is moving because the temperature gradients in front of the moving bubbles are much steeper than in front of a stationary bubble; thus, moving bubbles do not slow much before coalescing.

1. Introduction

Nucleate boiling occurs in many phenomena and is important in many industries. Ever since Nukiyama [1] first introduced the boiling curve and the different saturated pool boiling heat transfer regimes, there have been many studies of boiling heat transfer to clarify the fundamental boiling mechanisms. The many years of research on boiling have shown that boiling is a very complex process, far more complex than the descriptions given by classical theory. Researchers have sought for many years to understand the fundamental mechanisms of boiling, but have only begun to scratch the surface. Recent research on boiling in zero gravity has shown the importance of fundamental mechanisms that were previously thought to not be significant [2].

There have been various studies of the effects of bubble motion on a surface that illustrate how the bubble motion affects the heat transfer from the surface, with a few representative studies cited here to illustrate the importance of bubble motion on the heat transfer. Qiu and Dhir [3] experimentally studied the flow and heat transfer during bubble sliding on a heated surface to show the increased heat transfer due to the bubble motion. The analytical model of bubble motion along a heated wire by Christopher et al. [4] also illustrated the increased heat transfer due to the motion of a single bubble along a surface. Yan et al. [5] analyzed the effects of bubbles sliding along an inclined flat surface and a cylindrical surface on the heat transfer to show that the bubble movement increased the heat transfer. Sateesh et al. [6] also developed a model to predict the heat transfer around a bubble sliding on a vertical surface. Lu and Peng [7] presented a simplified algebraic model to describe the fundamental mechanisms driving bubble movements on a wire, with several key assumptions about the temperature profiles in the wire and around the bubble as well as several undetermined coefficients. Christopher et al. [8] and Wang et al. [9] observed bubble motions and jet flows, measured bubble velocities and simulated the temperature fields on microwires as single bubbles swept along a wire. They concluded that the Marangoni effect was the most important factor for the bubble motion. Christopher et al. [10] studied the bubble motion on a wire with a high-speed CCD and developed a phenomenological model to describe the motion of a single bubble.

The effects of bubble coalescence have also been studied extensively. The experimental investigation by Haddad and Cheung [11] of subcooled nucleate pool boiling showed the importance of this bubble coalescence of bubbles still attached to the surface at low heat fluxes, along with the bubble nucleation and growth stages. They noted that the coalescence of bubbles before departure can lead to formation of a vapor blanket on the surface. Dhir and his colleagues [12,13] used complex CFD models to analyze the dynamics of two or three bubbles coalescing on a heated surface to understand the conditions leading to coalescence. Chen and Chung [14] experimentally studied the coalescence of two adjacent bubbles still attached to the surface that were generated on adjacent microheaters and the effect of the coalescence on the heat transfer in the vicinity of the bubbles. The experimental study by Bonjour et al. [15] on the effect of coalescence before departure on the wall heat fluxes

* Corresponding author. Tel.: +86 10 6277 2986; fax: +86 10 6277 0209.
E-mail address: dmc@tsinghua.edu.cn (D.M. Christopher).

0017-9310/$ - see front matter © 2009 Elsevier Ltd. All rights reserved.
doi:10.1016/j.ijheatmasstransfer.2009.04.036

Nomenclature

c	specific heat, J/kg K
C	drag correction factor
D	diameter, m
e	minimum microlayer thickness, m
f	force, N
h	natural convection heat transfer coefficient, W/m^2 K
h_{fg}	latent heat, W/kg
L	contact line length, m
m	additional mass around bubble, kg
$\bar{M}$	molecular weight, kg/mol
Nu_D	Nusselt number = hD_w/λ_l
Pr	Prandtl number
q	heat transfer to bubble, W
q''	heat flux at wire surface, W/m^2
$\dot{Q}$	heat sink or source, W/m^3
R	radius, m
$\bar{R}$	ideal gas constant, J/kg K
Ra_D	Rayleigh number
Re	Reynolds number = $2\rho R_b U/\mu$
P	pressure, Pa
T	temperature, C or K
U	bubble velocity, m/s
x, y, z	coordinates, m
Greek	
α	proportionality constant
α_{evap}	evaporation heat transfer coefficient, W/m^2 K
Δy	distance from wire surface to bubble interface, m
Δz	element length in z-direction, m
γ	derivative of surface tension with respect to temperature, N/m K
λ	thermal conductivity, W/m K
μ	dynamic viscosity, Ns/m^2
θ	angular coordinate, rad
ρ	density, kg/m^3
σ	surface tension, N/m
σ_{evap}	evaporation coefficient
τ	time, s
ξ	moving coordinate, m
Subscripts	
0	base state
1	first bubble
2	second bubble
b	bubble
contact	contact force
d	drag
e	electrical heat source
evap	evaporation coefficient
i	interface
l	liquid
Marangoni	Marangoni force
sub	subcooling
sup	superheat
v	vapor
w	wire

during saturated nucleate pool boiling on a vertical wall showed that the coalescence increases the heat flow from the wall, but reduces the bubble departure frequency. Yang et al. [16] numerically analyzed bubble coalescence for various surface orientations. They successfully modeled coalescence of bubbles before departure and investigated the effects of various properties. Kolev [17] developed a model based on first principles to predict the conditions for which bubble interactions are important, especially the induced drag due to the motion of nearby bubbles, on an inclined surface for saturated boiling for a wide variety of conditions. Gjerkes and Golobic [18] measured the variation of the latent heat carried away by bubbles generated at two adjacent nucleation sites as a function of the distance between the sites to show that the energy transferred away from the surface by the bubbles decreases rapidly as the distance between the two sites decreases due to the interactions between nucleation sites including conduction in the wall and coalescence. Calka and Judd [19] did a similar study of the effects of the interactions between nucleation sites and found that the bubble formation was promoted by closely spaced nucleation sites with spacings less than the bubble departure diameter but was inhibited by site spacings larger than the bubble departure diameter. The observations of Kim et al. [20] of bubble interactions on a microheater in gravity showed that a large initial bubble formed which was then fed by smaller bubbles that nucleated underneath or very near the larger bubble and then coalesced with the larger bubble as they grew. Straub [2] discussed the importance of Marangoni convection for promoting bubble coalescence since the Marangoni convection controls the fluid flow very near the bubble interface which in turn affects the coalescence dynamics. The experimental observations of Sato et al. [21] of bubble growth and coalescence on artificial nucleation sites showed that bubble coalescence and the resulting convection increased the heat transfer from the surface in the vicinity of the nucleation sites.

The coalescence of bubbles after departure has also been studied. Narayanan et al. [22] developed a theoretical model to describe the coalescence of bubbles rising in a liquid based on the bubble shape and the type of wake. Shoji [23] studied the coalescence of noncondensable bubbles after departure from a single orifice to describe how the wake of a departing bubble affects the growth and departure of the next bubble. Zhang and Shoji [24] studied the interactions and coalescence between bubbles departing from two closely spaced artificial cavities as a function of the spacing between the bubbles. They found that the bubble coalescence near the surface after departure increases the bubble departure frequency. Son et al. [25] numerically analyzed the bubble merger process after departure or as the bubbles depart for bubbles generated from a single nucleation site to analyze the effect of coalescence on the vapor removal rate and the overall heat transfer. Legendre et al. [26] theoretically analyzed the interactions between two bubbles rising in a fluid to describe the conditions leading to coalescence.

This paper extends the mechanistic algebraic model of Marangoni convection driven bubble motion along a wire developed by Christopher et al. [10] to analyze the interactions among multiple bubbles. In this model, the driving temperature profile in the wire is calculated as a function of the heat transfer from the wire to the bubble. Christopher et al. [8] numerically solved the Navier–Stokes equations with the energy equation to describe the motion of a single bubble, but the extension of this method to two bubbles would be prohibitively expensive due to the need for very small elements between the bubble and the wire and for the very small time steps required by the VOF model. Thus, a practical, simplified model was developed to enable extensive analyses of the conditions leading to bubble coalescence rather than bubble repulsion on a thin wire. The results illustrate the nucleate boiling mechanisms that control the bubble dynamics and especially bubble coalescence on a sur-

face as the first step to the production of a vapor film and the transition to film boiling.

2. Theoretical description

2.1. Model analysis

During subcooled nucleate boiling, bubbles can sweep quickly across a surface. This motion is known to increase the heat transfer from the surface. Bubbles have been observed to sweep very quickly back and forth along a heated wire during subcooled nucleate boiling with high liquid subcoolings [9]. During boiling in normal gravity, the buoyancy and the natural convection due to the gravity normally have the greatest influence on the bubble growth, motion, and departure. However, Wang et al. [9] found that bubble sweeping is unique in that the gravitational effect is very small with bubble sweeping occurring on horizontal wires and up and down vertical wires. Thus, buoyancy and natural convection are not the mechanism driving the sweeping. A typical sweeping bubble is shown in Fig. 1. The steady-state bubble velocities for bubbles moving on platinum wires in water varied between 40 and 80 mm/s with the moving bubble sometimes stopping and reversing direction when meeting another bubble or sometimes coalescing.

This paper presents simulations of bubble sweeping and the relative motion between interacting bubbles. The temperature distribution in the wire is calculated by solving the conduction energy equation in the wire with the bubble velocities calculated from a force balance on the bubble that accounts for the Marangoni driving force, the inertia due to the added mass of liquid moving with the bubble, the drag due to the fluid and the wire and the surface tension force holding the bubble to the original nucleation site before the bubble begins to move. The model accurately predicts the bubble motion and the interactions including rebounding and coalescence.

2.2. Theoretical description

The geometry for two interacting bubbles is shown in Fig. 2. Both bubbles act as heat sinks in the wire, $\dot{Q}_{b1}(z)$ and $\dot{Q}_{b2}(z)$, as they travel along the wire. The wire is heated by a uniformly distributed heat source, $\dot{Q}_e$, and transfers energy to the liquid through natural convection. The effects of gravity and evaporation through the microlayer are neglected.

The conduction energy equation for the wire can be written as:

$$\rho c \frac{\partial T}{\partial \tau} = \lambda_w \frac{\partial^2 T}{\partial z^2} + \dot{Q}_e - \frac{h(T_w - T_b)2\pi R_w}{\pi R_w^2} - \dot{Q}_{b1}(z) - \dot{Q}_{b2}(z) \tag{1}$$

The bubbles are assumed to move in a viscous Newtonian liquid with the coordinate systems as shown in Fig. 2. The temperature gradient from the front of the bubble to the back of the bubble induces a thermal capillary force that drives the bubble motion. This Marangoni force drives the bubble towards the high temperature region. The Marangoni force acting on a bubble can be written as:

$$\begin{aligned} f_{Marangoni} &= -\int_0^{\pi} \frac{d\sigma}{dT_i}\left(\frac{\partial T_i}{R_b \partial \theta}\cdot \vec{k}\right) 2\pi R_b^2 \sin\theta d\theta \\ &= -\int_0^{\pi} \frac{d\sigma}{dT_i}\frac{\partial T_i}{R_b \partial \theta} 2\pi R_b^2 \sin^2\theta d\theta \end{aligned} \tag{2}$$

The temperature gradient on the bubble surface can be related to the temperature gradient in the z-direction on the interface by

$$\frac{\partial T_i}{R_b \partial \theta} = \frac{\partial T_i}{\partial x}\frac{dz}{R_b d\theta} = \frac{\partial T_i}{\partial z}\sin\theta \tag{3}$$

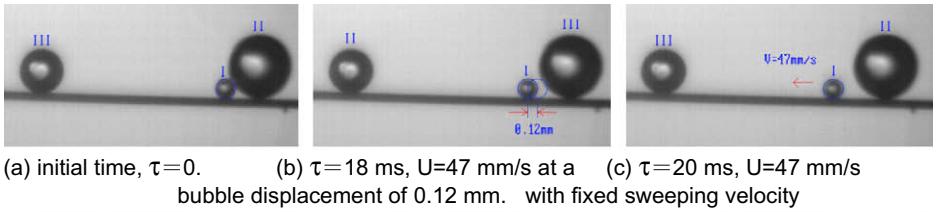

(a) initial time, τ=0. (b) τ=18 ms, U=47 mm/s at a bubble displacement of 0.12 mm. (c) τ=20 ms, U=47 mm/s with fixed sweeping velocity

(d) τ=60 ms, bubble decelerates to 0 mm/s within 0.15 mm, stays for 1 ms, then reverses direction (e) τ=70 ms, U=47 mm/s with fixed sweeping velocity. (f) τ=110 ms, bubble is stationary.

Fig. 1. Bubble sweeping back and forth along a wire between two fixed bubbles (q'' = 879 kW/m^2, T_l = 46.8 °C, 1000 fps). (a) Initial time, t = 0. (b) τ = 18 ms, U = 47 mm/s at a bubble displacement of 0.12 mm. (c) τ = 20 ms, U = 47 mm/s with fixed sweeping velocity. (d) τ = 60 ms, bubble decelerates to 0 mm/s within 0.15 mm, stays for 1 ms, then reverses direction. (e) τ = 70 ms, U = 47 mm/s with fixed sweeping velocity. (f) τ = 110 ms, bubble is stationary.

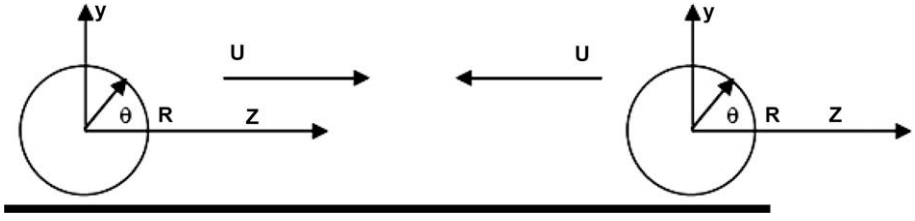

Fig. 2. Coordinate systems around the bubbles.

The temperature gradient on the interface, $\frac{\partial T_i}{\partial z}$, in Eq. (3), is then a function of the height on the bubble. The average temperature gradient on the interface can be assumed to be related to the temperature gradient in the wire as:

$$\frac{dT_i(y)}{dz} = \alpha \frac{\partial T_w}{\partial z} \tag{4}$$

where α is a proportionality constant to be determined later. The surface tension variation with temperature along the interface can be expressed as:

$$\sigma(T_i) = \sigma(T_0) - \gamma(T_i - T_0) \tag{5}$$

where $\sigma(T_0)$ is the interfacial tension at temperature T_0 and γ is a positive constant for most fluids. With a moving coordinate system, $\xi = z - U^* t$ that is moving with the bubble velocity U, the Marangoni driving force can be written as:

$$f_{Marangoni} = 2\pi\alpha\gamma R_b^2 \int_0^{\pi} \frac{\partial T_w}{\partial z} \sin^3\theta d\theta = 2\pi\alpha\gamma R_b \int_{-R_b}^{R_b} \frac{\partial T_w}{\partial \xi}\left(1 - \frac{\xi^2}{R_b^2}\right) d\xi \tag{6}$$

The viscous force on a slowly moving vapor bubble moving in an infinite liquid pool is given by the Hadamard–Rybczynski law [27,28]:

$$f_d = -4\pi\mu R_b u \tag{7}$$

However, since this force applies to a bubble moving in an infinite liquid pool and does not take into account the drag on the bubble due to the wire, it underestimates the drag force on the wire. Therefore, the drag on a typical bubble was calculated by solving the Navier–Stokes equations for a bubble moving along a wire. The results in Fig. 3 show that the drag is primarily a function of the Reynolds number and is not strongly related to the relative sizes of the wire and the bubble. The drag forces calculated from the CFD analysis were then correlated relative to the Hadamard–Rybczynski drag as:

$$C = \begin{cases} 1.70 + 0.0261Re - 0.000112Re^2 & \text{for } Re < 45.7 \\ 2.19 + 0.0102Re & \text{for } Re > 45.7 \end{cases} \tag{8}$$

where the total drag force is then given by:

$$f_d = -4\pi\mu R_b u^* C \tag{9}$$

When the bubble is moving, the contact force between the bubble interface and the wire will be zero due to the thin microlayer existing between the bubble and the wire. Numerous researchers have observed such microlayers between bubbles and the adjacent surfaces. Observations of moving bubbles on wires have also indicated that a thin microlayer develops between the bottom of the bubble and the wire that is several micrometers thick. However, when the bubble is stationary and the interface is connected to a nucleation site, a force exists between the bubble and the surface due to surface tension between the interface and the surface which can be expressed by:

$$f_{contact} = 2\sigma L_{\text{contact}} \cos(\theta) \tag{10}$$

where σ is the liquid surface tension, θ is the contact angle, and $L_{contact}$ is the length of the contact line where the bubble interface contacts the surface, assumed to be on the order of the size of a typical nucleation site, about 1 μm. A sensitivity study showed that this assumption had negligible effect on the results. When $f_{contact} \geqslant f_{Marangoni}$, $U = 0$. The bubble heat source term was then calculated by assuming that the heat transfer from the wire to the bubble was mainly due to conduction since the velocities in the microlayer region underneath the bubble are quite small. Thus, the heat transfer can be given by:

$$q(z) = 2\int_0^{R_b} \lambda_l \frac{\Delta T_{sup}(z)}{\Delta y + \frac{\lambda_l}{\alpha_{evap}}} dx \Delta z \tag{11}$$

where ΔT_{sup} is the superheat in the wire (the temperature difference between the wire and the saturation temperature inside the bubble), Δz is the width of a computational element along the wire and α_{evap} is the evaporation heat transfer coefficient given by [29]:

$$\alpha_{evap} = \frac{2\sigma_{evap}}{2 - \sigma_{evap}} \frac{\rho_v h_{fg}^2}{T_v} \sqrt{\frac{\bar{M}}{2\pi\bar{R}T_v}} \left(1 - \frac{P_v}{2h_{fg}\rho_v}\right) \tag{12}$$

The distance from the wire to the bubble interface which is a function of both x and z is:

$$\Delta y = e + R_w - \sqrt{R_w^2 - x^2} + R_b - \sqrt{R_b^2 - x^2 - z^2} \tag{13}$$

where e is the microlayer thickness, R_w is the wire radius, and R_b is the bubble radius. The heat source term in the wire due to this heat transfer would then be:

$$\dot{Q}_b(z) = \frac{q(z)}{\pi R_w^2 \Delta z} \tag{14}$$

As a bubble accelerates in a liquid, the acceleration depends on the additional mass of liquid that accelerates with the bubble. Lamb [30] showed that the volume of the additional mass is equal to one half of the bubble volume. Therefore, the additional mass is:

$$m = \frac{1}{2}\rho_l \frac{4}{3}\pi R_b^3 \tag{15}$$

The bubble motion when $f_{Marangoni} > f_{contact}$ is then calculated from Newton's law:

$$m\frac{dU}{dt} = f_{Marangoni} - f_d \tag{16}$$

The natural convection heat transfer coefficient in Eq. (1) was calculated from the correlation recommended by Churchill and Chu [31]:

$$Nu_D = \left\{0.60 + \frac{0.387Ra_D^{1/6}}{[1 + (0.559/Pr)^{9/16}]^{8/27}}\right\}^2 \tag{17}$$

where D is the wire diameter.

2.3. Numerical simulation

The temperature field was calculated by solving the energy equation, Eq. (1), with the bubble velocities calculated by solving Eq. (16) once $f_{Marangoni} \geqslant f_{contact}$. The heated wire was assumed to be smooth so that the contact force only developed at the initial bubble position when the bubble was not moving. The wire radius

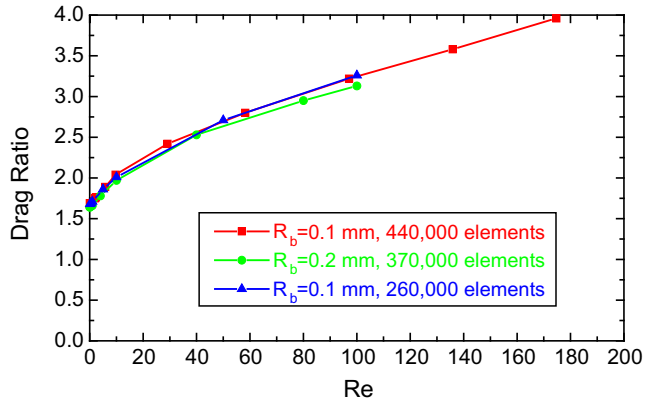

Fig. 3. Ratio of the drag on a bubble moving along a wire to the Hadamard–Rybczynski solution.

was assumed to be 0.05 mm and the microlayer thickness, e, was assumed to be 1 μm. Since experimental observations have shown that the bubble motion only occurs for rather large subcoolings, the liquid was assumed to have rather large subcoolings of 20–40 °C. The wire was assumed to be either platinum or 316 stainless steel with the liquids being either water or ethanol near the boiling point with a contact angle of $\theta = 20°$.

Eq. (1) was solved on a one-dimensional grid in the z-direction with a step size of 0.005 mm and 4000 elements. The time step was 10^{-6} s. The equation was solved using second-order central differences for the diffusion term and the implicit method for the transient term. The algebraic equations were then solved directly with the TDMA method so there were no iterations. The solution of Eq. (11) used 10 elements in the x-direction (the radial direction) with a grid size of 0.005 mm. Twice as many elements in both directions and smaller time steps, 2×10^{-7} s, resulted in relative changes to the interaction times and locations of less than 0.05%. The bubbles were initially placed far enough apart so that they reached steady-state velocities before interacting.

3. Results

3.1. Individual bubble dynamics

3.1.1. Moving bubble velocity

Typical heat fluxes during nucleate boiling are in the range of 10^5–10^6 W/m^2, so typical heat generation rates in the wire are between 4×10^9 and 4×10^{10} W/m^3. For water with a liquid subcooling of 40 °C and a wire superheat far from the bubble of 10 °C, the heat generation rate needed to balance the natural convection in the absence of bubbles from Eq. (17) was approximately $\dot{Q}_e = 1.45 \times 10^{10}$ W/m^3. The calculated steady-state bubble velocity for these conditions on a platinum wire was $u = 54.5$ mm/s for $R_b = 0.2$ mm which agrees with the range of bubble velocities observed experimentally [9]. The results in Fig. 4 show that larger bubbles move somewhat faster and that bubbles move more slowly in ethanol than in water. The results in Fig. 4 also show that the bubbles accelerated very quickly, within about 50 ms in ethanol and about 150 ms in water. All these results agree with experimental observations. In ethanol, the predictions show that the bubbles initially overshoot the steady-state velocity and then quickly return to a steady-state value. The overshoot is due to both the momentum of the additional mass around the bubble and that the wire temperature distribution does not develop instantaneously, so the bubble experiences a somewhat higher temperature difference driving the Marangoni flow as it accelerates, which then decreases slightly as the acceleration decreases. This overshoot is more obvious in the ethanol where the bubbles accelerate faster.

The steady-state bubble velocities are functions of various parameters. Fig. 5 shows the variation of the steady-state velocity for various liquid subcoolings for bubbles moving on a 0.1 mm diameter platinum wire. The results show that the velocity increases dramatically as the superheating increases. Also, there is a critical minimum superheat below which the bubbles do not move. This was also observed experimentally with minimum bubble velocities of about 30 mm/s in water and about 15 mm/s in ethanol. The subcooling had a much smaller effect on the bubble velocities. The superheat has a larger effect because higher superheats increase the evaporation heat transfer into the bubble which increases the temperature gradients in the wire (and, hence, into the bubble) which increases the Marangoni driving force. The velocities in ethanol are much lower because of the property differences with smaller velocities for smaller bubbles as observed in Fig. 4.

3.1.2. Effect of wire properties

Fig. 6 shows the effect of the wire properties on the steady-state bubble velocities for bubbles moving in water with a subcooling of 20 °C. The bubbles on the stainless steel wire move much faster

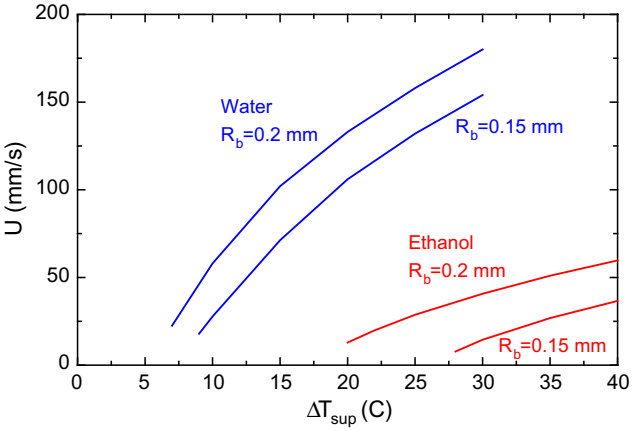

Fig. 5. Steady-state bubble velocities for various superheats on a platinum wire with a subcooling of 20 °C.

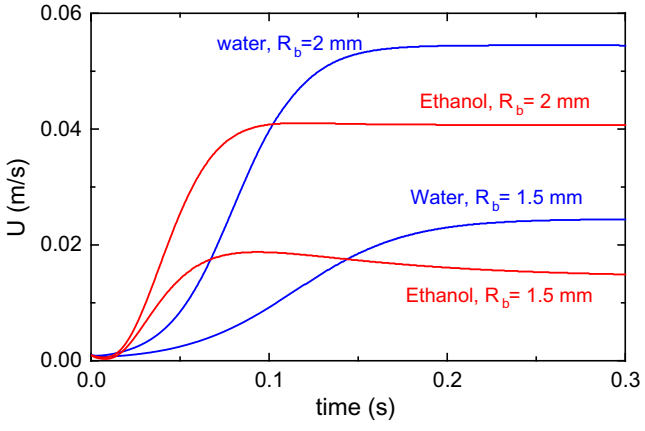

Fig. 4. Individual bubble velocities without interactions on a 0.1-mm diameter platinum wire. For ethanol, $\Delta T_{sub} = 20$ °C and $\Delta T_{sup} = 30$ °C, for water, $\Delta T_{sub} = 40$ °C and $\Delta T_{sup} = 10$ °C.

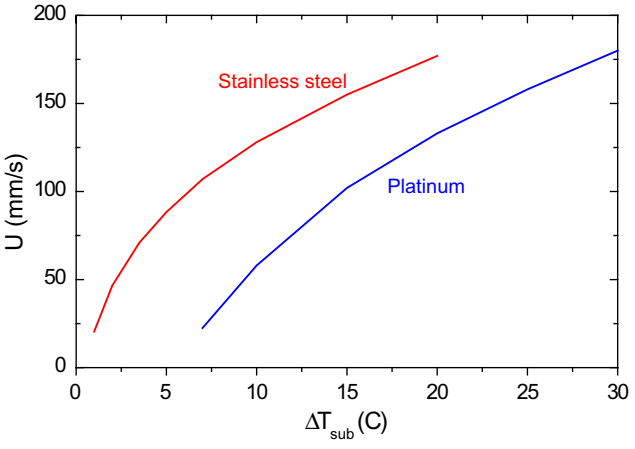

Fig. 6. Effect of wire properties on the steady-state bubble velocities for bubble motion in water with a subcooling of 20 °C.

than on the platinum wire because of the different thermal diffusivities of the two materials. Since the thermal diffusivity of platinum is about seven times that of stainless steel, the heat transfer in the stainless steel is much slower, so the temperature gradient across the bubble is much greater, which increases the Marangoni driving force and the bubble velocity.

3.1.3. Temperature distributions in the wire

Stationary and moving bubbles create different temperature distributions in the wire due to their different heat transfer distributions. The temperature distributions for stationary and moving 0.2 mm bubbles are shown in Fig. 7a for water with a subcooling of 20 °C and a superheat of 10 °C and in Fig. 7b for ethanol with a subcooling of 20 °C and a superheat of 30 °C (so that the velocities and temperature drops are similar because for the same superheat, a bubble moves much slower in ethanol as shown in Fig. 5). The temperatures underneath the stationary bubbles are much lower than underneath the moving bubbles, especially for the stainless steel wire. The temperature distributions for the stationary bubble are symmetric while those for the moving bubble have a very steep leading edge and a long trailing edge as the uniform heating increases the wire temperature again after the bubble passes. The unsymmetrical temperature distribution results in higher temperatures on the front surface of the bubble and lower temperatures on the back surface which creates the Marangoni driving force in the horizontal direction. The differences between the stationary and moving temperature distributions are much more pronounced with the stainless steel wire because it has a much smaller thermal diffusivity than the platinum. These temperature distributions were found to control the types of bubble interactions since large velocities tend to result in more bubble coalescence.

3.2. Multi-bubble interactions

3.2.1. One bubble moving towards another stationary bubble

Fig. 8a shows the displacement history of a 0.2 mm radius bubble moving along a platinum wire towards another stationary 0.2 mm stationary bubble in water with a subcooling of 40 °C and a superheat of 14 °C. For these conditions, the two bubbles do not coalesce but the oncoming bubble slows and reverses direction as it approaches the stationary bubble. This has often been seen in experiments where moving bubbles rarely coalesced with stationary bubbles [32]. The locations plotted on the ordinates in Fig. 8

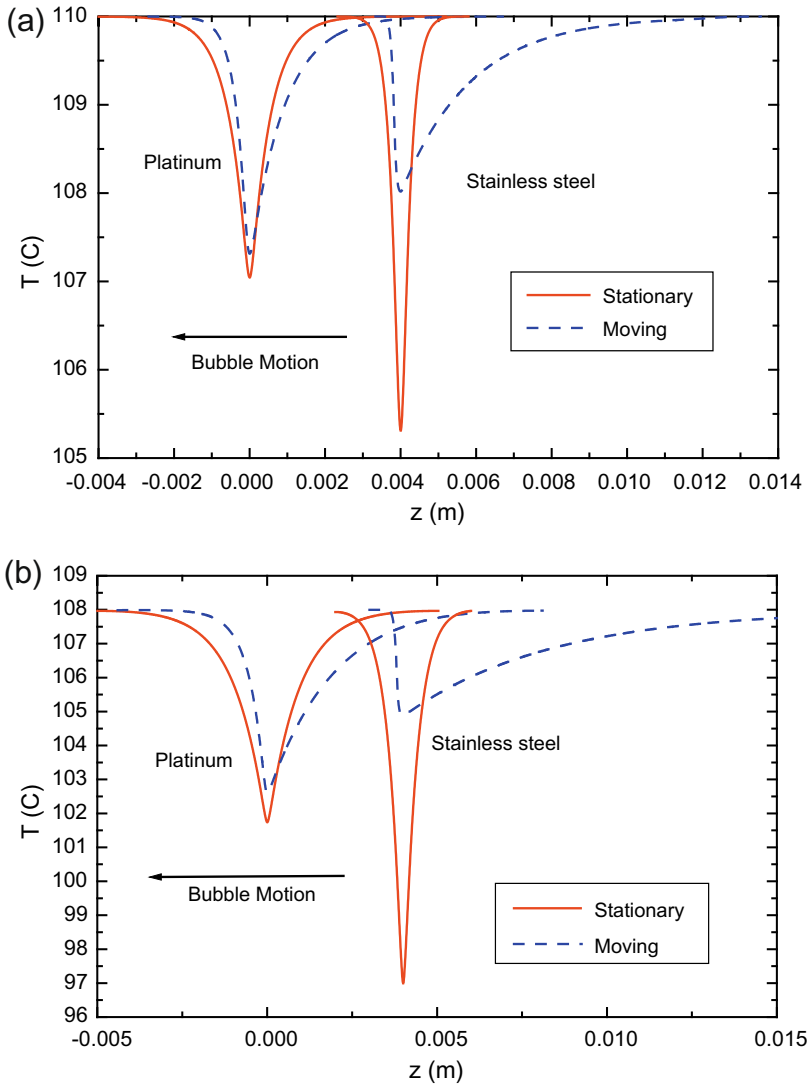

Fig. 7. Temperature profiles in platinum and stainless steel wires during bubble motion of a 0.2-mm radius bubble in (a) water with subcooling of 20 °C and superheat of 10 °C and (b) in ethanol with subcooling of 20 °C and superheat of 30 °C. (a) Water, (b) ethanol.

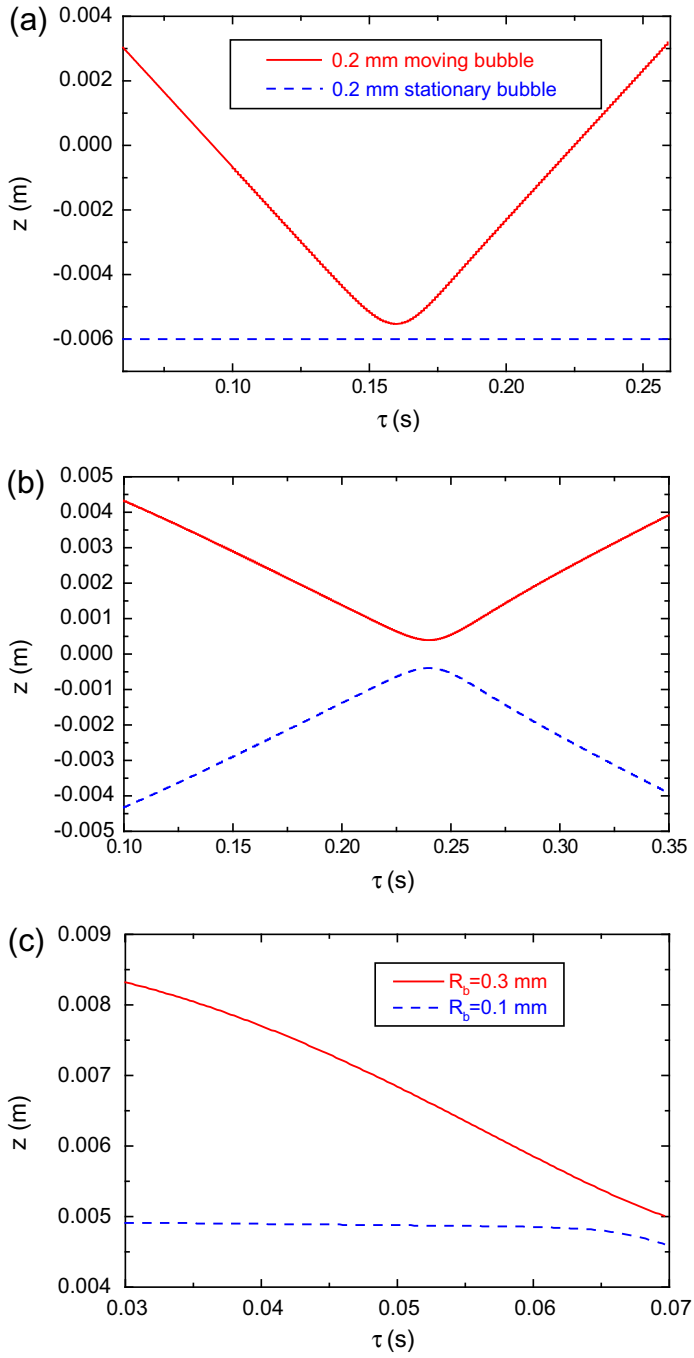

Fig. 8. Bubble displacements for bubbles moving on a platinum wire in water with a subcooling of 40 °C. (a) Bubble moving towards a stationary bubble with a superheat of 14 °C, (b) two 0.2 mm radii bubbles moving toward each other with a superheat of 8 °C, (c) two bubbles moving in the same direction with a superheat of 13 °C.

are the centers of the bubbles with coalescence assumed to occur when the distance between centers was equal to the sum of the two bubble radii; thus, coalescence occurs before the lines meet. The moving bubble slows as it approaches the stationary bubble because it encounters the cooler wire temperatures produced by the presence of the stationary bubble. As shown in Fig. 7, the wire temperatures are depressed for many bubble radii from the bubble, for the example in Fig. 7a, the wire temperature is depressed by a full 1 °C for more than 3 bubble radii from the stationary bubble center on the platinum wire. As the moving bubble encounters this cooler region, the temperature difference across the bubble decreases and the bubble eventually stops. At this point the temperatures behind the bubble are now higher rather than lower than the temperatures in front of the bubble so the bubble reverses direction and begins moving towards the hotter region in the other direction as shown in Fig. 8a. As shown by the bubble interaction maps in Section 3.3, at higher velocities (higher superheats), the bubbles coalesce since the moving bubble has a higher velocity and more momentum, so the two bubbles coalesce even though the oncoming bubble slows as it approaches the stationary bubble. In some cases, the stationary bubble begins to move away from the approaching bubble because the temperature distribution around the stationary bubble is no longer symmetric as the other bubble approaches. The unsymmetrical temperature distribution creates a Marangoni force that begins moving the stationary bubble once the Marangoni force overcomes the contact force in Eq. (10).

3.2.2. Two bubbles moving towards each other

Fig. 8b shows the displacement histories for two 0.2 mm radius bubbles moving towards each other on a platinum wire in water with a subcooling of 40 °C and a superheat of 8 °C. The bubbles started far apart and moved at a constant velocity for some time before interacting. As they approach each other, they both slow as they move into the reduced temperatures in front of the oncoming bubble. For these conditions, the inertia cannot overcome the reversal of the Marangoni forces as the bubbles approach and the bubbles reverse direction. As shown in Section 3.3, for higher superheats which create higher bubble velocities, the higher inertias result in the bubbles coalescing. Experimentally, bubbles are normally seen to coalesce when moving towards each other [32]. The bubbles normally coalesce when both are moving because they do not slow much as they approach each other since the temperature gradients in front of moving bubbles are quite steep as shown in Fig. 7 so the Marangoni force is not significantly reduced.

3.2.3. Two bubbles initially moving in the same direction

Fig. 8c shows the displacement histories for two different size bubbles, 0.3 and 0.1 mm radii, moving in the same direction. When the rear bubble is larger than the lead bubble, the rear bubble will be faster and will eventually catch up to the lead bubble and will coalesce at higher superheats with larger bubbles. This has often been observed experimentally when the rear bubble is much larger than the lead bubble. As Fig. 8c shows, initially the larger bubble moves at its equilibrium speed until it gets close to the smaller lead bubble. Then, since the smaller bubble has already absorbed some energy from the wire, the wire temperature will be depressed and the larger bubble will slow some. At the same time, because the rear bubble is depressing the wire temperature close to the lead bubble, the lead bubble is experiencing a larger temperature difference so it accelerates. For the case shown in Fig. 8c, the velocity of the larger bubble is still greater than that of the smaller bubble so they eventually coalesce. A 0.25 mm radius bubble requires a much larger superheat to catch up to and coalesce with a 0.1 mm bubble. A 0.2 mm radius bubble came very close to but did not coalesce with a 0.1 mm radius bubble, with both eventually moving at the same rate in the same direction a short distance apart.

3.3. Bubble interaction maps

The bubble dynamics depend on a variety of conditions, including the bubble sizes, solid and liquid properties, and the wire and liquid temperatures. Fig. 9 gives regime maps for some of the various interaction dynamics as a function of the bubble size and the superheat for bubbles moving on platinum wires in water. Fig. 9a shows the interaction results for one bubble moving towards another stationary equal size bubble. For smaller bubbles and smaller superheats, the bubbles did not move along the wire as indicated in Figs. 5 and 6. For moderate superheats, the moving bubble reverses direction as it approaches the depressed temperatures in the vicinity of the stationary bubble. The momentum of the additional mass around the bubble carries the bubble into the cooler region, but the bubble then reverses direction and moves back towards the warmer region. At higher superheats, the higher velocities of the moving bubble carry the bubble close enough to the stationary bubble to create a sufficiently unsymmetrical temperature field around the stationary bubble which in turn creates enough Marangoni force to overcome the contact force and cause the stationary bubble to begin moving in the same direction as the initially moving bubble. When the bubbles are sufficiently large (or the superheats sufficiently high), the arriving bubble catches up to and coalesces with the now moving bubble after a short distance. Fig. 9b shows the interaction regime map for two

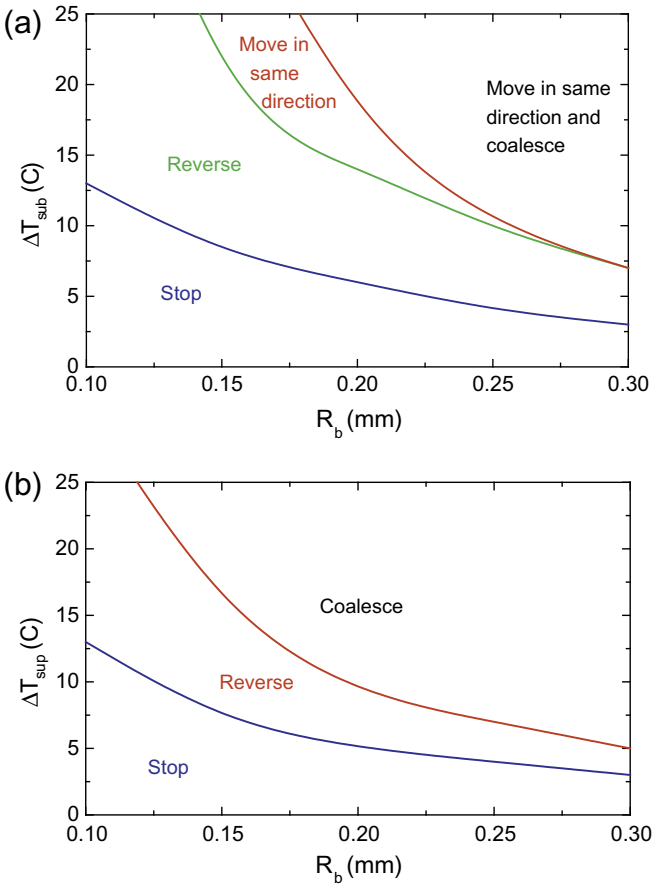

Fig. 9. Dynamic interaction regime maps for bubbles moving on platinum wires in water with 40 °C subcooling. (a) One bubble moving toward a stationary equal size bubble and (b) two equal size bubbles moving towards each other.

equal size bubbles moving towards each other. At moderate superheats, the bubbles reverse direction as they approach each other and encounter the cooler wire temperatures due to the other bubble. At higher superheats, the moving bubbles coalesce as their larger momentums carry them into each other. The superheats required for two moving bubbles to coalesce are smaller than for a moving bubble to coalesce with a stationary bubble since the temperature gradients in front of a moving bubble are steeper than in front of a stationary bubble as shown in Fig. 7. When a smaller bubble approaches a larger stationary bubble, the smaller bubble reverses direction except for systems with very high superheats where the larger bubble begins to move and then quickly moves away from the smaller bubble. When a larger bubble approaches a smaller stationary bubble, the larger bubble will reverse direction at moderate superheats and coalesce at very large superheats.

4. Conclusions

A phenomenological model was developed to predict bubble motion and bubble interactions along a heated wire during subcooled nucleate boiling. The model takes into account the heat transfer from the wire to the bubble, the Marangoni driving force due to the temperature difference across the bubble interface from front to back, the wire temperature distribution, and the drag and contact forces acting on the bubble. The model accurately predicts the steady-state bubble velocities for bubbles sweeping along a heated wire. The model also shows that when a moving bubble approaches a stationary bubble at lower superheats, the reduced temperatures around the stationary bubble force the moving bub-

ble to reverse direction, as has been observed experimentally. At higher superheats, the moving bubble will coalesce with the stationary bubble. The model also shows that when two moving bubbles are approaching each other from opposite directions, they are more likely to collide and coalesce because the temperature gradients in front of the bubbles are much steeper so that they do not cause the bubbles to slow much before they collide. Thus, the model accurately characterizes the conditions for which bubbles tend to coalesce and for which they tend to repel each other.

Acknowledgement

This project was supported by the National Natural Science Foundation of China (Contract No. 50636030).

References

[1] S. Nukiyama, The maximum and minimum values of heat transmitted from metal to boiling water under atmospheric pressure, J. Jpn. Soc. Mech. Eng. 37 (1934) 367–374 (Translated in Int. J. Heat Mass Transfer 9 (1966) 1419–1433).
[2] J. Straub, Microscale boiling heat transfer under 0g and 1g conditions, Int. J. Thermal Sci. 39 (2000) 490–497.
[3] D. Qiu, V.K. Dhir, Experimental study of flow pattern and heat transfer associated with a bubble sliding on downward facing inclined surfaces, Exp. Thermal Fluid Sci. 26 (6–7) (2002) 605–616.
[4] D.M. Christopher, H. Wang, X.F. Peng, Dynamics of bubble motion and bubble top jet flows from moving vapor bubbles on microwires, J. Heat Transfer 127 (2005) 1260–1268.
[5] Y.Y. Yan, D. Kenning, K. Cornwell, Sliding and sticking vapor bubbles under inclined plane and curved surfaces, Int. J. Refrig. 20 (8) (1997) 583–591.
[6] G. Sateesh, S.K. Das, A.R. Balakrishnan, Analysis of pool boiling heat transfer: effect of bubbles sliding on the heating surface, Int. J. Heat Mass Transfer 48 (8) (2005) 1543–1553.
[7] J.F. Lu, X.F. Peng, Bubble slippage on thin wires during subcooled boiling, Int. J. Heat Mass Transfer 49 (2006) 2337–2346.
[8] D.M. Christopher, H. Wang, X.F. Peng, Numerical analysis of the dynamics of moving vapor bubbles, Int. J. Heat Mass Transfer 49 (2006) 3626–3633.
[9] H. Wang, X.F. Peng, B.X. Wang, D.Z. Lee, Bubble sweeping mechanisms, Sci. China (E) 46 (3) (2003) 225–233.
[10] D.M. Christopher, J. Jiang, L. Zhang, Phenomenological model for bubble sweeping, in: Proceedings of the 18th International Symposium on Transport Phenomena, Daejeon, Korea, 2007, pp. 667–674.
[11] K.H. Haddad, F.B. Cheung, Steady-state subcooled nucleate boiling on a downward-facing hemispherical surface, J. Heat Transfer 120 (1998) 365–370.
[12] A. Mukherjee, V.K. Dhir, Study of lateral merger of vapor bubbles during nucleate pool boiling, J. Heat Transfer 126 (2004) 1023–1039.
[13] V.K. Dhir, H.S. Abarajith, D. Li, Bubble dynamics and heat transfer during pool and flow boiling, Heat Transfer Eng. 28 (7) (2007) 608–624.
[14] T.L. Chen, J.N. Chung, Coalescence of bubbles in nucleate boiling on microheaters, Int. J. Heat Mass Transfer 45 (11) (2002) 2329–2341.
[15] J.M. Bonjour, M. Clausse, M. Lallemand, Experimental study of the coalescence phenomenon during nucleate pool boiling, Exp. Thermal Fluid Sci. 20 (2000) 180–187.
[16] Z.L. Yang, T.N. Dink, R.R. Nourgaliev, B.R. Sehgal, Numerical investigation of bubble coalescence characteristics under nucleate boiling condition by a lattice-Boltzmann model, Int. J. Thermal Sci. 39 (2000) 1–17.
[17] N.I. Kolev, The influence of mutual bubble interaction on the bubble departure diameter, Exp. Thermal Fluid Sci. 8 (1994) 167–174.
[18] H. Gjerkes, Il. Golobic, Measurement of certain parameters influencing activity of nucleation sites in pool boiling, Exp. Thermal Fluid Sci. 25 (2002) 487–493.
[19] A. Calka, R.L. Judd, Some aspects of the interaction among nucleation sites during saturated nucleate boiling, Int. J. Heat Mass Transfer 28 (12) (1985) 2331–2342.
[20] J. Kim, J.F. Benton, D. Wisniewski, Pool boiling heat transfer on small heaters: effect of gravity and subcooling, Int. J. Heat Mass Transfer 45 (2002) 3919–3932.
[21] T. Sato, Y. Koizumi, H. Ohtake, Experimental study on fundamental phenomena of boiling using heat transfer surfaces with well-defined cavities created by MEMS (effect of spacing between cavities), J. Heat Transfer 130 (2008) 084501.
[22] S. Narayanan, L.H.J. Goossens, N.W.F. Kossen, Coalescence of two bubbles rising in line at low Reynolds numbers, Chem. Eng. Sci. 29 (1974) 2071–2082.
[23] M. Shoji, Nonlinear bubbling and micro-convection at a submerged orifice, Tsinghua Sci. Technol. 7 (2) (2002) 97–108.
[24] L. Zhang, M. Shoji, Nucleation site interaction in pool boiling on the artificial surface, Int. J. Heat Mass Transfer 46 (2003) 513–522.
[25] G. Son, N. Ramanujapu, V.K. Dhir, Numerical simulation of bubble merger process on a single nucleation site during pool nucleate boiling, J. Heat Transfer 124 (1) (2002) 51–62.
[26] D. Legendre, J. Magnaudet, G. Mougin, Hydrodynamic interactions between two spherical bubbles rising side by side in a viscous liquid, J. Fluid Mech. 497 (2003) 133–166.
[27] J.S. Hadamard, Mouvement permanent lent d'une sphere liquide et visqueuse dans un liquide visqueux, C.R. Acad. Sci. Paris 152 (1911) 1735–1738.
[28] W. Rybczynski, Uber die fortschreintende bewegung einer flussigen kugel in einem zahen medium, Bull Intern. Acad. Sci. Cracovie Ser. A Sciences Mathematiques 1 (1911) 40.
[29] V.P. Carey, Liquid–Vapor Phase-Change Phenomena, Hemisphere, Washington, 1992.
[30] H. Lamb, Hydrodynamics, sixth ed., Dover, 1945.
[31] S.W. Churchill, H.H.S. Chu, Correlating equations for laminar and turbulent free convection from a horizontal cylinder, Int. J. Heat Mass Transfer 18 (1975) 1049.
[32] L. Zhang, D.M. Christopher, Microscale vapor bubble interactions during subcooled nucleate boiling on a heated wire, in: Proceedings of MNC2007 MicroNanoChina07, Sanya, Hainan, China, 2007.